Materials Horizons

ROYAL SOCIETY OF CHEMISTRY

COMMUNICATION

View Article Online
View Journal | View Issue

Cite this: *Mater. Horiz.*, 2026, **13**, 4950

Received 26th January 2026,
Accepted 27th March 2026

DOI: 10.1039/d6mh00147e

rsc.li/materials-horizons

Interface-governed electromechanical coupling in bioinspired hierarchical piezoelectric poly(L-lactide) architectures

Martina Žabčić, [ab] Lea Gazvoda,[a] Masoumeh Sepideh Salehidashtbayaz,[c] Ita Junkar,[d] Selestina Gorgieva, [e] Andraž Rešetič, [f] Matjaž Spreitzer [a] and Marija Vukomanović *[a]

Bioinspired materials frequently derive functionality from hierarchical organization and chemically active interfaces that mediate the conversion of mechanical stimuli into biological signals. Emulating such interface-governed mechanotransduction in synthetic soft matter remains a major challenge for electromechanical biomaterials. Here, we introduce a hierarchical piezoelectric polymer architecture in which plasma-engineered interfaces act as active functional elements that govern ultrasound-driven electromechanical coupling. Two piezoelectric poly(L-lactide) (PLLA) layers with distinct morphologies—a uniaxially drawn film and an electrospun fibrous mat—are directly bonded *via* plasma-assisted surface activation, enabling morphologically well-integrated and strong interfacial adhesion without additional adhesive phases. Under ultrasound excitation, mechanical energy is preferentially concentrated at the chemically activated interface, generating enhanced shear deformation and a synergistically amplified piezoelectric response that exceeds the performance of the individual layers. This interface-dominated electromechanical coupling translates efficiently to biological systems through an extracellular-matrix-mimetic fibrous surface, enabling effective transfer of electrically mediated cues to adherent cells. Ultrasound-activated piezostimulation of human keratinocytes demonstrates enhanced cell adhesion, proliferation, and cytoskeletal organization. By establishing chemically programmed interfaces as a new design axis for electromechanical energy transduction, this work defines a bioinspired materials chemistry paradigm for adaptive piezoelectric surfaces and interfaces with broad relevance to bioelectronics, regenerative medicine, and dynamic tissue engineering.

New concepts

This work introduces an interface-governed design paradigm for soft piezoelectric materials, demonstrating that chemically activated interfaces can dominate electromechanical coupling under ultrasound excitation, rather than acting as passive boundaries between functional layers. Inspired by biological mechanotransduction, where mechanical signals are processed through hierarchical structures and heterogeneous interfaces, the study reveals how plasma-engineered interfacial adhesion within a layered piezoelectric architecture concentrates shear deformation and amplifies piezoelectric response beyond that of individual components. The resulting interface-driven electromechanical coupling enables efficient generation and transfer of electrical cues through an extracellular-matrix-mimetic fibrous surface, promoting effective communication with adherent cells under non-invasive ultrasound stimulation. By shifting piezoelectric optimization from bulk composition, filler loading, and crystallinity toward interfacial chemistry, mechanical coupling, and architectural design, this approach establishes a general and scalable materials chemistry framework for adaptive, bioinspired electromechanical interfaces. The concept is broadly applicable to shear-active piezoelectric polymers and multilayer soft electronic systems, opening new directions for bioelectronics, regenerative medicine, and dynamic tissue-engineering platforms.

Introduction

Bioinspired materials frequently exploit hierarchical organization and interfacial coupling to convert mechanical stimuli into functional biological signals.[1] In native extracellular matrices (ECM), mechanical forces are transduced through multiscale architectures and heterogeneous interfaces, enabling electrically and chemically mediated regulation of cell behaviour.[2]

[a] *Advanced Materials Department, Jožef Stefan Institute, Jamova cesta 39, Ljubljana 1000, Slovenia. E-mail: marija.vukomanovic@ijs.si*
[b] *Jožef Stefan International Postgraduate School, Jamova cesta 39, Ljubljana 1000, Slovenia*
[c] *Biotechnical Faculty, University of Ljubljana, Jamnikarjeva ulica 101, 1000 Ljubljana, Slovenia*
[d] *Department of Surface Engineering, Jožef Stefan Institute, Jamova cesta 39, Ljubljana 1000, Slovenia*
[e] *Faculty of Mechanical Engineering, University of Maribor, Smetanova ulica 17, 2000 Maribor, Slovenia*
[f] *Condensed Matter Physics Department, Jožef Stefan Institute, Jamova cesta 39, Ljubljana 1000, Slovenia*

Replicating such mechano–electrical interactivity in synthetic materials remains a central challenge for next-generation bioelectronics and regenerative systems.

Stimuli-responsive biomaterials have therefore attracted increasing attention as platforms capable of sending, receiving, and responding to cellular signals, offering new routes for controlling critical processes such as cell adhesion, migration, proliferation, and differentiation during tissue regeneration.[3–5]

Among external stimuli, ultrasound (US) is particularly attractive due to its non-invasive nature and deep tissue penetration. US-responsive piezoelectric biomaterials can convert mechanical deformation into electrical polarization, enabling contact-mediated stimulation of cells without implanted electrodes.[6,7] However, achieving efficient and biologically relevant signal transduction requires not only optimized piezoelectric response, but also intimate interfacial contact between the material and living cells.

Poly(L-lactide) (PLLA) is one of the few biodegradable and biocompatible polymers exhibiting intrinsic piezoelectricity.[8] Its electromechanical response is strongly governed by crystallinity, chain orientation, and molecular conformation.[9] Owing to its helical chain structure—analogous to that found in natural macromolecules such as proteins and DNA[10]—PLLA exhibits its strongest piezoelectric response under shear deformation.[11,12] This characteristic makes PLLA particularly well suited for US-driven activation, where shear strains dominate in soft and layered structures.

Existing strategies to enhance PLLA piezoelectricity have primarily focused on optimizing bulk structure, including uniaxial drawing, annealing, incorporation of high-aspect-ratio fillers, and nanostructuring.[9,13–16] While these approaches can improve crystallization and chain orientation, they typically address piezoelectric performance at the level of individual components. Importantly, they overlook the potential role of interfacial electromechanical coupling between mechanically dissimilar but electrically active layers—a principle widely exploited in natural hierarchical systems,[17] yet largely unexplored in organic piezoelectric materials.

Nanostructuring PLLA into electrospun fibrous networks offers additional advantages by increasing surface area and mimicking ECM-like topography, thereby improving cell adhesion and guidance.[18–20] However, nanostructured PLLA surfaces are inherently hydrophobic, which limits effective cell–material contact.[21,22] Moreover, previously reported multilayer PLLA systems rely on soft adhesive interlayers, such as poly(caprolactone), which mechanically decouple the layers and prevent cooperative electromechanical response.[18] As a result, synergistic piezoelectric enhancement through layer–layer interaction has not been achieved.

Here, we propose a bioinspired hierarchical piezoelectric architecture in which a uniaxially drawn PLLA film and an electrospun fibrous mat are directly bonded *via* plasma-assisted surface activation, enabling strong interfacial adhesion without additional adhesive phases (illustrated in Fig. 1).[23] Under ultrasound excitation, direct coupling of these mechanically dissimilar layers induces adhesion-mediated electromechanical coupling, enhancing shear-driven polarization and synergistic piezoelectric response while simultaneously promoting efficient signal transfer to cells through a plasma-modified fibrous biointerface.

In contrast to conventional strategies that enhance piezoelectricity through bulk crystallinity or molecular orientation, this work establishes an interface-governed design paradigm in which chemically activated interfaces act as primary sites of

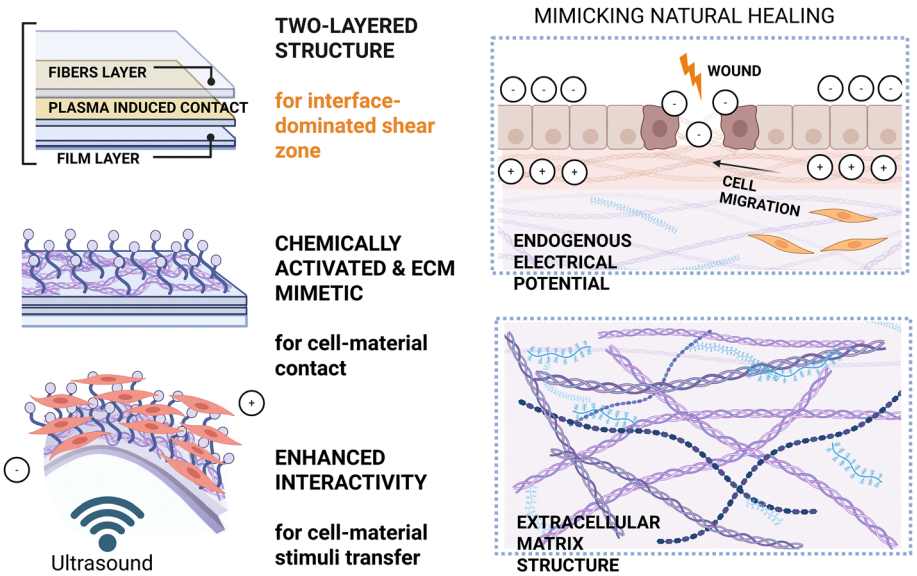

Fig. 1 The main concept of interactive piezo-PLLA design, is based on: two-layered structure designed to provide electromechanical coupling which will increase the piezoelectricity and provide enhanced stimuli signal as well as charged and textured surface for improved cell–material contact, both following enhanced interactivity for efficient transferring the signal to cells and their response, due to the structure which mimics the charge –driven interactions of cells with ECM fibrous structure during natural healing.

electromechanical transduction. Inspired by biological mechanotransduction, this approach defines a materials chemistry frontier for soft piezoelectric systems, where emergent functionality arises from architectural and interfacial design rather than compositional complexity.

Results and discussion

By combining piezoelectricity with biodegradability and biocompatibility, PLLA represents an attractive platform for interactive bioelectronic materials. However, achieving effective interactivity in piezo-PLLA systems requires not only optimized piezoelectric performance as the source of electrical stimulation, but also a surface architecture that enables intimate and efficient contact with living cells. Considering the limitations of previously developed piezo-PLLA morphologies,[8,24] we designed a bioinspired hierarchical architecture composed of two directly bonded piezoelectric layers with distinct morphologies: a smooth, uniaxially drawn film and a textured electrospun fibrous mat (Fig. 1). This design mimics charge-driven interactions between cells and the fibrous extracellular matrix during natural healing, where endogenous electrical potentials and hierarchical structure play a central role.[25] High-aspect-ratio fillers (hydroxyapatite and bacterial cellulose nanofibers)[13,26] were incorporated into both layers to enhance their intrinsic piezoelectricity, while plasma-assisted surface activation enabled strong direct adhesion between the layers. Under ultrasound excitation, this direct interfacial contact promotes synergistic electromechanical coupling, generating enhanced shear deformation and amplified piezoelectric output. The resulting electrical signal is efficiently transferred to cells through the hydrophilic, plasma-treated fibrous top layer, which serves both as an ECM-mimicking biointerface and as a conduit for effective signal exchange between the material and biological systems.

Surface and interface properties in two-layered structures

A strong and stable interface between the smooth PLLA HAp films and the PLLA fibrous layers was achieved by plasma-assisted surface activation followed by mechanical pressing. Atmospheric-pressure plasma, a cold plasma technique widely used for biomedical surface modification, enables controlled tuning of surface chemistry and wettability through the introduction of polar functional groups.[27–29] Here, this strategy was exploited to enable direct bonding between two chemically identical but morphologically distinct PLLA layers that otherwise show no intrinsic adhesion.

Plasma treatment transformed the PLLA surface from hydrophobic to hydrophilic, with a morphology-dependent response. Owing to nanostructuring, electrospun PLLA fibres were initially more hydrophobic than smooth films (Fig. 2b), but both surfaces became hydrophilic after plasma activation, with statistically significant reductions in contact angle ($p < 0.001$ for fibres and $p < 0.0001$ for films). Despite this shift, the intrinsic difference between films and fibres was preserved, indicating that nanostructure continues to influence surface wettability after chemical activation.

Changes in surface chemistry were confirmed by cationic methylene blue staining[30] which revealed a pronounced increase in anionic functional groups on plasma-treated films and fibres (Fig. 2a). The enhanced staining of PLLA BC_{CMC} fibres reflects the combined contribution of plasma-induced oxygen-containing groups and carboxyl functionalities originating from carboxymethylated bacterial nanocellulose exposed at the fibre surface. XPS analysis corroborated these findings, showing an increased concentration of oxygen-containing species consistent with COO^- and C–O groups (Fig. 2c).

This chemically activated interface enabled robust mechanical adhesion between the two layers upon pressing, whereas no bonding was observed without plasma pre-treatment (Fig. 2d and Fig. S1), and the adhesion remained stable upon plasma aging. The activated interfacial chemistry (Fig. 2e) therefore plays a critical role in establishing direct layer–layer contact, which underpins the electromechanical coupling discussed below. Beyond improving wettability or adhesion, plasma activation serves here as a chemical tool to program interfacial functionality, enabling mechanical energy concentration and electromechanical signal amplification at bonded polymer interfaces.

Crystallinity and chain orientation in two-layered structures

Two-layer architectures were designed with either aligned or randomly oriented fibrous top layers (Fig. 2e). These consisted of a uniaxially drawn PLLA HAp film combined with either co-drawn PLLA BC_{CMC} fibres (PLLA HAp DR5/BC_{CMC} DR5 fibres) or non-drawn PLLA BC_{CMC} fibres deposited onto the pre-drawn film (PLLA HAp DR5/BC_{CMC} fibres). Their structural properties were compared with those of the corresponding single-layer films and fibrous mats.

Both bilayer architectures predominantly contained the α′-PLLA phase, with the characteristic diffraction maximum at 16.4° (Fig. 3a). Previous studies have shown that thermal treatment and uniaxial stretching of semicrystalline PLLA can induce partial transformation of the α phase into the β phase,[31] particularly in the presence of anisotropic fillers.[13] Consistent with this, incorporation of a small amount (1 wt%) of high-aspect-ratio fillers (HAp rods or cellulose nanofibres), combined with co-drawing of the bilayer, led to the appearance of an additional diffraction peak at 28.8° in PLLA HAp DR5/BC_{CMC} DR5 fibres, indicating the formation of a β-PLLA phase (Fig. 3a).

DSC-determined crystallinity of PLLA in the drawn PLLA HAp DR5 film was significantly higher than that in electrospun PLLA BC_{CMC} fibres ($p < 0.05$, Fig. 3d). In the bilayer systems, co-drawing of the fibrous layer did not result in statistically significant changes in overall crystallinity, indicating that the crystalline contribution is dominated by the bulk film. All samples exhibited melting temperatures in the narrow range of 182–183 °C, and both single-layer fibres and bilayer structures showed pronounced cold crystallization relative to the PLLA HAp film (Fig. S2), suggesting additional crystallization potential within the fibrous phase.

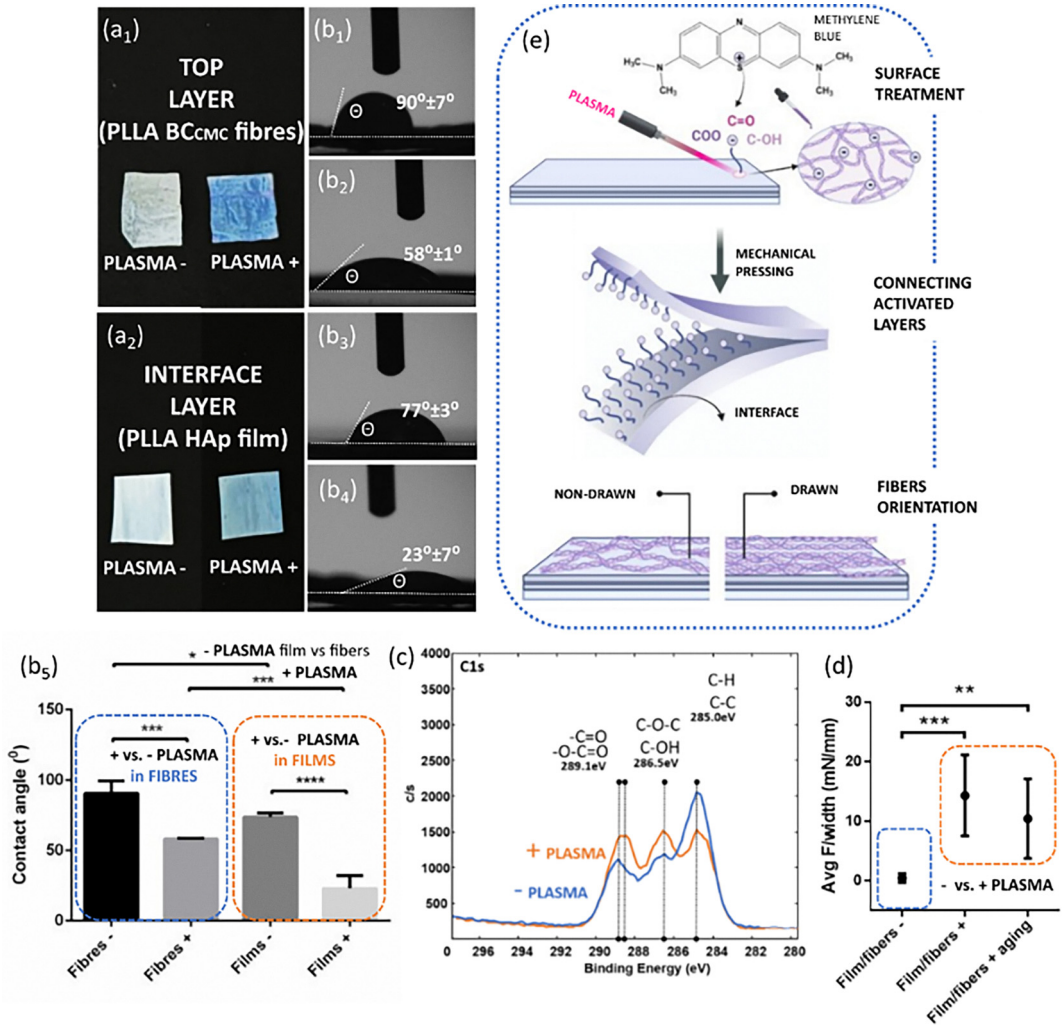

Fig. 2 Surfaces and interface in two-layered PLLA structures. Methylene blue (MB) staining of PLLA BC_{CMC} fibres and PLLA HAp smooth films with and without plasma treatment (a_1–a_2); water contact angles at the surface of films and fibres and statistically relevant differences induced by nanostructuring and plasma (b_1–b_5); XPS spectra of PLLA surface before and after plasma treatment (c); adhesion between layers following plasma activation, and plasma stability (aging) (d), toward two-layered structure: surface activation, connecting activated layers and fibers orientation at the top (e), *, **, *** and **** indicate $p < 0.05$, $p < 0.005$, $p < 0.001$ and $p < 0.0001$, respectively.

In contrast to crystallinity, fibre drawing had a pronounced effect on molecular orientation. SAXS patterns revealed strong anisotropic orientation in uniaxially drawn PLLA HAp DR5 films, whereas non-drawn PLLA BC_{CMC} fibres exhibited isotropic scattering, consistent with randomly oriented crystalline domains (Fig. 3c). When the film and fibres layers were directly bonded and co-drawn, a joint directional alignment of crystalline domains with enhanced long-range order was observed.

Chain orientation was quantified by polarized Raman spectroscopy using the intensity ratio of the ν(C–COO) band measured parallel and perpendicular to the drawing direction (Fig. 3b). As expected, single-layer electrospun fibres showed no bulk orientation (Fig. 3e). In contrast, co-drawn bilayers (PLLA HAp DR5/BC_{CMC} DR5 fibres) exhibited significantly higher overall PLLA orientation than both single-layer fibres ($p < 0.001$) and the drawn PLLA HAp film alone ($p < 0.005$). Notably, bilayers prepared by depositing non-drawn fibres onto pre-drawn films showed no additional increase in orientation compared to the film alone, indicating that co-drawing is required for fibre contribution to macromolecular alignment.

Overall, these results demonstrate that strong bond at the interface following co-drawing fibres on top of the bulk film enables enhanced PLLA chain orientation in directly bonded bilayer architectures.

Piezoelectric properties of two-layered structures

Similar to other polymers with a helical chain conformation, PLLA exhibits dominant shear piezoelectricity.[7,15] Mechanical deformation of the films was induced by US stimulation at 80 kHz (low frequency) and 1 MHz (high frequency), the latter also being relevant for therapeutic ultrasound applications.[6] The US-activated piezoelectric response was strongly frequency dependent. At 80 kHz, all samples exhibited relatively low peak-to-peak (p–p) voltage outputs, whereas stimulation at 1 MHz

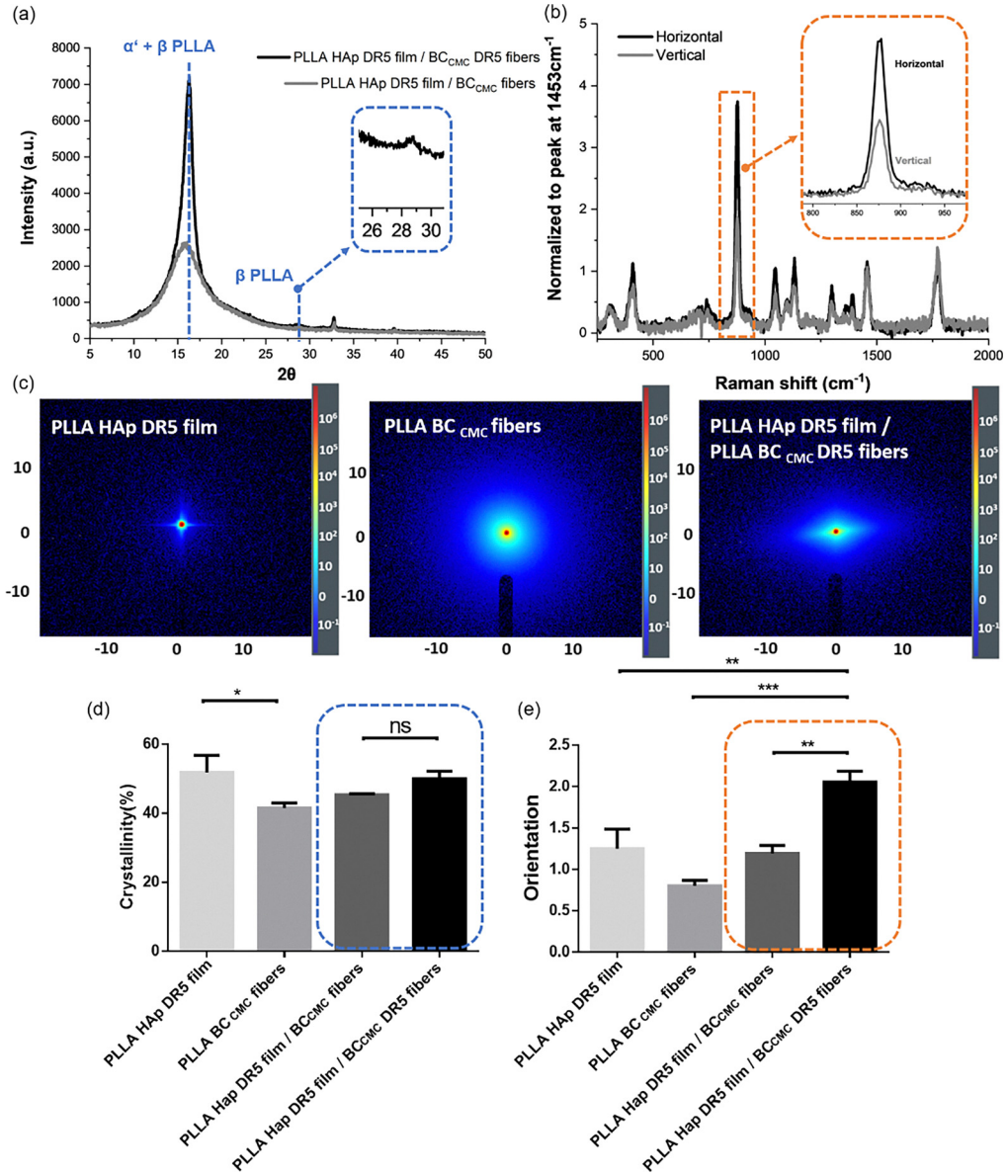

Fig. 3 Crystallization and orientation of two-layer structures: XRD patterns showing phase composition in two-layered structures (a); polarized Raman spectra for PLLA HAp DR5 film/BC$_{CMC}$ DR5 fibres showing molecular orientation (b); SAXS 2D patterns showing orientation of crystalline domains in f PLLA HAp DR5 film, PLLA BC$_{CMC}$ fibers and co-drawn PLLA HAp DR5 film/BC$_{CMC}$ DR5 fibres (c); DSC- determined crystallinity (d); Raman- determined chain orientation (e), *, **and *** indicate $p < 0.05$, $p < 0.005$ and $p < 0.001$, respectively.

resulted in a significant increase in p–p voltage for all investigated materials ($p < 0.0001$; Fig. 4b and Table S1).

For single-layer materials, the uniaxially drawn PLLA HAp DR5 film generated substantially higher p–p voltages than the electrospun PLLA BC$_{CMC}$ fibrous mat under both 80 kHz ($p < 0.001$) and 1 MHz ($p < 0.0001$) stimulation. This behaviour correlates well with the higher crystallinity and stronger chain orientation of PLLA in the drawn film compared with the randomly oriented electrospun fibres (Fig. 3).

A more pronounced enhancement was observed in the bilayer architectures, whose piezoelectric responses exceeded those of both single-layer components and could not be explained solely by differences in crystallinity or molecular orientation. Despite the higher orientation in bilayers with co-drawn fibres, both bilayer configurations exhibited significantly higher p–p voltages (and respective charge densities, Fig. S3) than the single-layer film and fibre samples under US activation at both 80 kHz ($p < 0.001$ and $p < 0.005$ for bilayers with non-drawn and drawn fibres, respectively) and 1 MHz ($p < 0.0001$ for all bilayer *vs.* single-layer comparisons) (Fig. 4b and c). These results indicate the emergence of a synergistic electromechanical response arising from the joint activation of the directly connected layers.

The possibility of triboelectric signal generation was carefully evaluated through dedicated control measurements (Fig. S4), particularly taking into account measuring set up in which

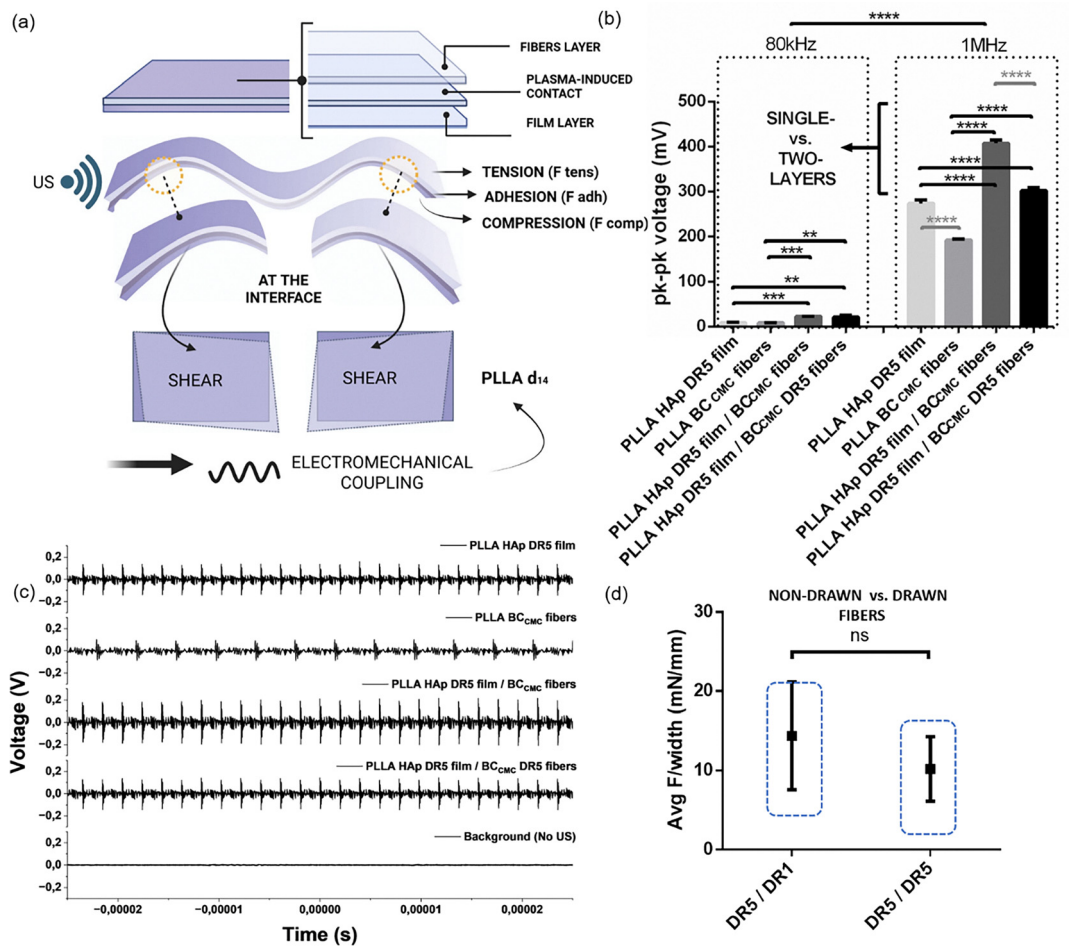

Fig. 4 The piezoresponces in single and two-layered PLLA structures: the main principle of detected electromechanical coupling in directly connected piezoelectric layers obtained after activation with US (a); p–p values after 80 kHz and 1 MHz US activation (b); piezoresponse signal at 1 MHz (comparison of the single- (PLLA HAp DR5 and PLLA BC_{CMC} fibres) with drawn and non-drawn two- layered structures (PLLA HAp DR5 film/BC_{CMC} DR5 fibres and PLLA HAp DR5 film /BC_{CMC} fibres, respectively) relative to the background without US activation) (c); adhesion forces in drawn and non-drawn two separated-layered structures (d), **, *** and **** indicate $p < 0.005$, $p < 0.001$ and $p < 0.0001$, respectively.

Kapton tape (as tribo- negative layer) is covering PLLA (as tribo-positive).[32] However, as shown in Fig. S4$c_{1–3}$, no measurable triboelectric response was detected either between the individual PLLA layers or between the bilayer and Kapton tape confirming that the voltage output observed under ultrasound activation originates from the intrinsic piezoelectric response of the material.

To verify the interfacial enhancement effect, three additional multilayer structures with different interlayer connections were designed: strong (plasma-induced), weak (mechanically pressed) and non-connected (intermediate layer) (Fig. S5). The measured voltage output followed the interlayer bonding strength, with the lowest output observed for the sample containing the intermediate layer, comparable to the individual layers, as also obtained in recent study when PLLA layers were separated by electro-inert interlayer,[18] confirming that stronger interfacial bonding induces greater interfacial strain under US-driven deformation and enhances electromechanical coupling.

To further assess the mechanical stability of the material and the temporal stability of its voltage output, bilayer samples with and without electrodes were immersed in liquid and continuously stimulated with 80kHz US (Fig. S6a). The response was first evaluated by periodically switching the US on and off (Fig. S6b and Video S1, S2) and testing signal after increasing the US power (Video S3), while the one-minute interval over 40 min measurement demonstrated stable signal generation throughout the experiment (Fig. S6c and Video S4), with no evidence of delamination at the plasma-bonded interface (Fig. S6d).

Because the chemical composition of both layers and their surfaces prior to bonding was identical, as well as due to the absence of the coupling in case of bilayer with integrated interlayer, the observed differences between bilayer configurations are attributed primarily to differences in interfacial mechanical coupling. This is reflected in the higher p–p voltages observed for bilayers with non-drawn fibres compared to those with co-drawn fibres ($p < 0.0001$; Fig. 4). Peel-off measurements confirmed stronger interfacial adhesion in bilayers with non-drawn fibres, where the plasma-induced bonding was preserved, whereas co-drawing after plasma treatment reduced the adhesion strength (Fig. 4d and Fig. S1).

The direct correlation between interfacial adhesion strength and piezoelectric output demonstrates that strong mechanical coupling between layers is critical for efficient electromechanical interaction. Enhanced adhesion promotes more effective strain transfer across the interface, thereby amplifying shear deformation and resulting in a synergistically increased piezoelectric response under ultrasound activation.

The electromechanical coupling observed in these bilayer architectures is attributed to shear deformation predominantly generated during ultrasound (US) activation of directly bonded piezoelectric layers. Numerical modelling has identified shear strain as the dominant mode of deformation induced by US in soft, laminar structures typical of flexible electronic systems.[33] Consistent with this, ultrasonic techniques are widely used for non-destructive evaluation of adhesive joints in thermoplastics, where the interaction of US waves with bonded interfaces is particularly sensitive to interfacial shear strength and integrity.[34,35]

In layered materials exhibiting shear piezoelectricity, such as PLLA, US activation is therefore expected to be especially effective. However, achieving efficient electromechanical coupling requires intimate and mechanically robust interfacial contact. Upon US excitation, mechanical deformation is transferred toward the interface between layers with dissimilar mechanical properties. In the present system, the stiffer PLLA HAp film is bonded to the more compliant PLLA BC_{CMC} fibrous layer *via* plasma-induced direct contact. US excitation induces bending of the bilayer, while differences in mechanical compliance generate interfacial friction, leading to localized shear strain concentrated at the interface, as predicted previously.[33]

When two piezoelectric layers with contrasting mechanical characteristics are strongly bonded, US activation thus couples bending deformation with interfacial friction, resulting in amplified shear strain and synergistic shear piezoelectricity. The combined effects of mechanical support between layers, plasma-enabled interfacial adhesion, and efficient shear deformation under US excitation critically govern the piezoelectric response of the bilayer structures (Fig. 4a and b). This mechanism is clearly reflected in the higher piezoelectric output of bilayers with non-drawn fibres, which exhibit stronger interfacial contact, compared to those with co-drawn fibres. In PLLA HAp DR5/BC_{CMC} fibres, a 26% increase in peak-to-peak voltage was observed relative to PLLA HAp DR5/BC_{CMC} DR5 fibres, indicating that improved interfacial contact enables more effective shear deformation. These results reveal an interface-dominated electromechanical coupling mechanism, in which plasma-induced adhesion transforms the interface from a passive boundary, occurring in case of presence of electroneutral interlayer,[18] into an active site of US-induced shear-mediated polarization. Notably, the magnitude of the piezoelectric response correlates more strongly with interfacial adhesion strength than with crystallinity or molecular orientation, underscoring the central role of interface chemistry in governing electromechanical function.

Furthermore, because the transmission and reflection of US waves at material interfaces are frequency dependent,[35] the strength of electromechanical coupling and the resulting piezoelectric response increase with the frequency of US activation, consistent with the experimentally observed enhancement at 1 MHz.

Morphology of two-layered structures

SEM examination of layered structure revealed distinct and well-defined morphologies. As described above, during fabrication the surface of the bulk film and the surface of the electrospun fibre mat—intended to form the interface—were first treated with atmospheric plasma and subsequently mechanically pressed to ensure intimate interfacial contact. This process enabled effective integration of the two morphologically different layers (Fig. $5a_1$). Initial, adhesion- free structure contains morphologically well-integrated layers, obtained after plasma pre-treatment (Fig. $5a_1$ and Fig. S7). To enable detailed inspection of the individual layers and their interface, partial delamination was intentionally introduced, as indicated in Fig. $5a_2$.

Cross-sectional SEM images clearly show two distinct layers: a smooth bottom bulk film and a top layer composed of sub-micrometre-thick fibres (Fig. $5a_2$). The bottom film exhibits an internal layered structure, arising from the presence of a filler during uniaxial drawing, consistent with previous observations.[13] The fibrous top layer shows partial fibre fusion, which is most likely a consequence of mechanical pressing during the lamination process.

Top-view SEM analysis further highlights pronounced morphological differences depending on the drawing protocol. In the PLLA HAp DR5 film/BC_{CMC} DR5 fibres system, where fibres were uniaxially drawn together with the film, a clear preferential fibre alignment along the drawing direction is observed. In contrast, for the PLLA HAp DR5 film/BC_{CMC} fibres system—where fibres were deposited onto an already drawn film—the fibres exhibit a random orientation (Fig. S8).

Beyond modifying surface chemistry, plasma treatment is known to influence surface morphology, including roughness and porosity.[29] Fibres that were not plasma-treated exhibit lower porosity and smaller pore sizes (Fig. $5b_1$ and b_2), characteristic of solvent-induced porosity commonly formed during electrospinning. In this process, rapid evaporation of a highly volatile solvent from the polymer jet leads to the formation of porous fibres. In contrast, fibres subjected to additional plasma treatment display increased porosity and larger pore sizes (Fig. $5c_1$ and c_2), indicating plasma-induced surface modification.

Materials with finer microstructures[36] and enhanced porosity[37] are widely reported to promote improved cell attachment, as surface roughness facilitates cell adhesion and spreading. Moreover, the introduction of internal closed porosity within piezoelectric polymer fibres may positively influence their electromechanical performance by reducing relative permittivity.[38] However, excessive porosity can adversely affect macroscopic polarization and compromise mechanical integrity.[39] In the present system, plasma-induced morphological changes are largely confined to the fibre surface, while the fibre bulk remains free of open pores. Consequently, mechanical stability remains sufficient to withstand ultrasound-induced deformation,

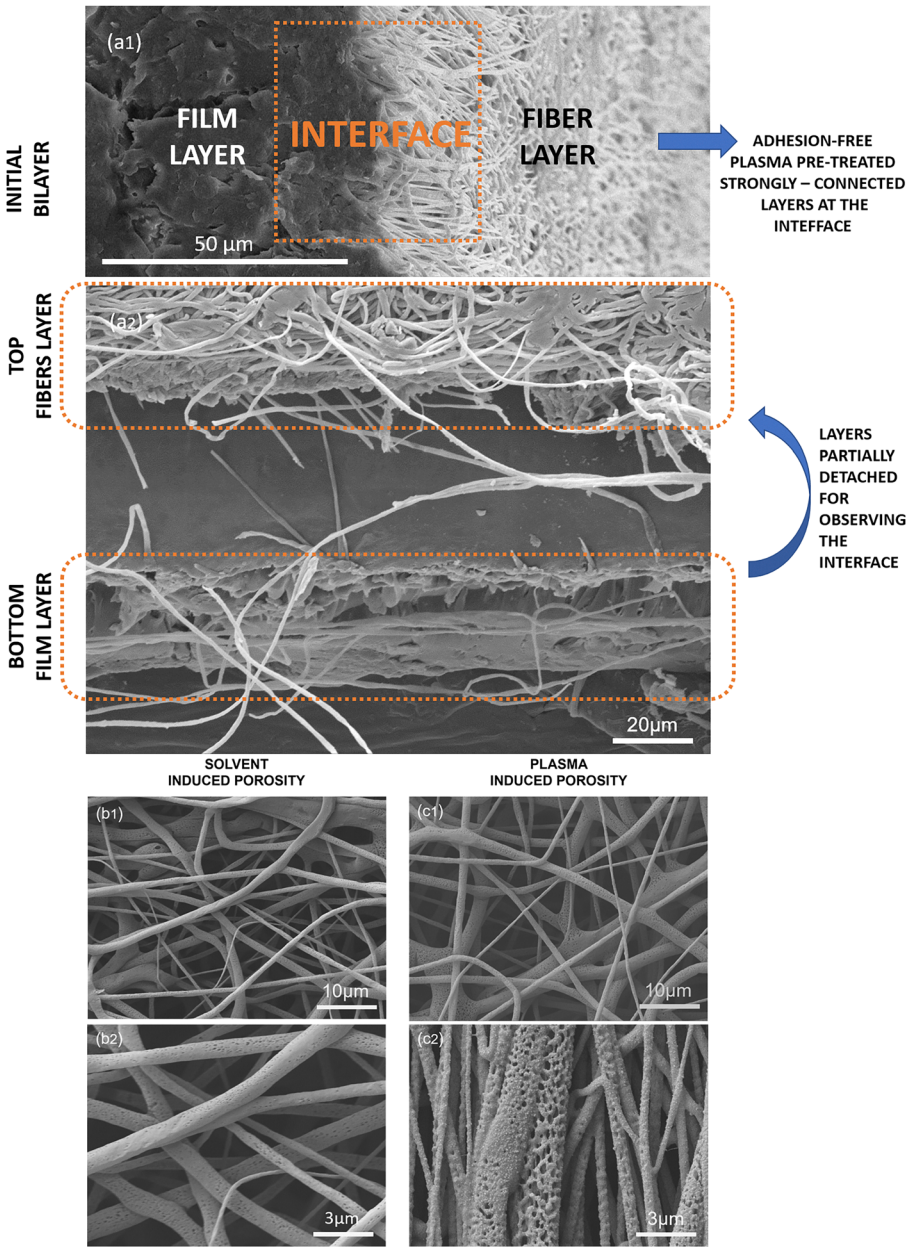

Fig. 5 SEM morphology of two-layered structure: adhesion-free, plasma pre-treated bilayer before (a1) and after (a2) separation of previously connected layers, the interface between bottom film layer and top fibres layer is visible (a); the top fibers layer shows surface roughness and porosity, including solvent- induced porosity (b1 and b2) and plasma- induced porosity (c1 and c2).

and no significant degradation of piezoelectric performance due to plasma-induced porosity was detected. In contrast, the influence of smaller, solvent-induced pores is expected to be more pronounced. Overall, achieving an optimal balance between surface porosity for enhanced cell–material interactions and minimal open porosity for preserved piezoelectric functionality is essential for maximizing material performance.

Interactivity of two-layered structures: HaCaT cell adhesion and piezostimulated growth

Cellular responses are used as a functional readout of interface-mediated electromechanical coupling and signal transfer efficiency. Plasma treatment increased surface polarity and wettability, transforming hydrophobic PLLA surfaces into hydrophilic ones (Fig. 2), while simultaneously inducing morphological changes in the fibrous layer, including increased surface roughness and porosity (Fig. 5). Together, these chemical and topographical modifications enhanced material interactivity, beginning with cell–surface attachment (Fig. 6a).

Plasma-treated fibrous substrates showed significantly increased HaCaT cell adhesion compared to untreated counterparts ($p < 0.05$; Fig. 6b). Even without plasma activation, cells preferentially adhered to fibrous surfaces over smooth films, reflecting the higher surface area and favourable topography of

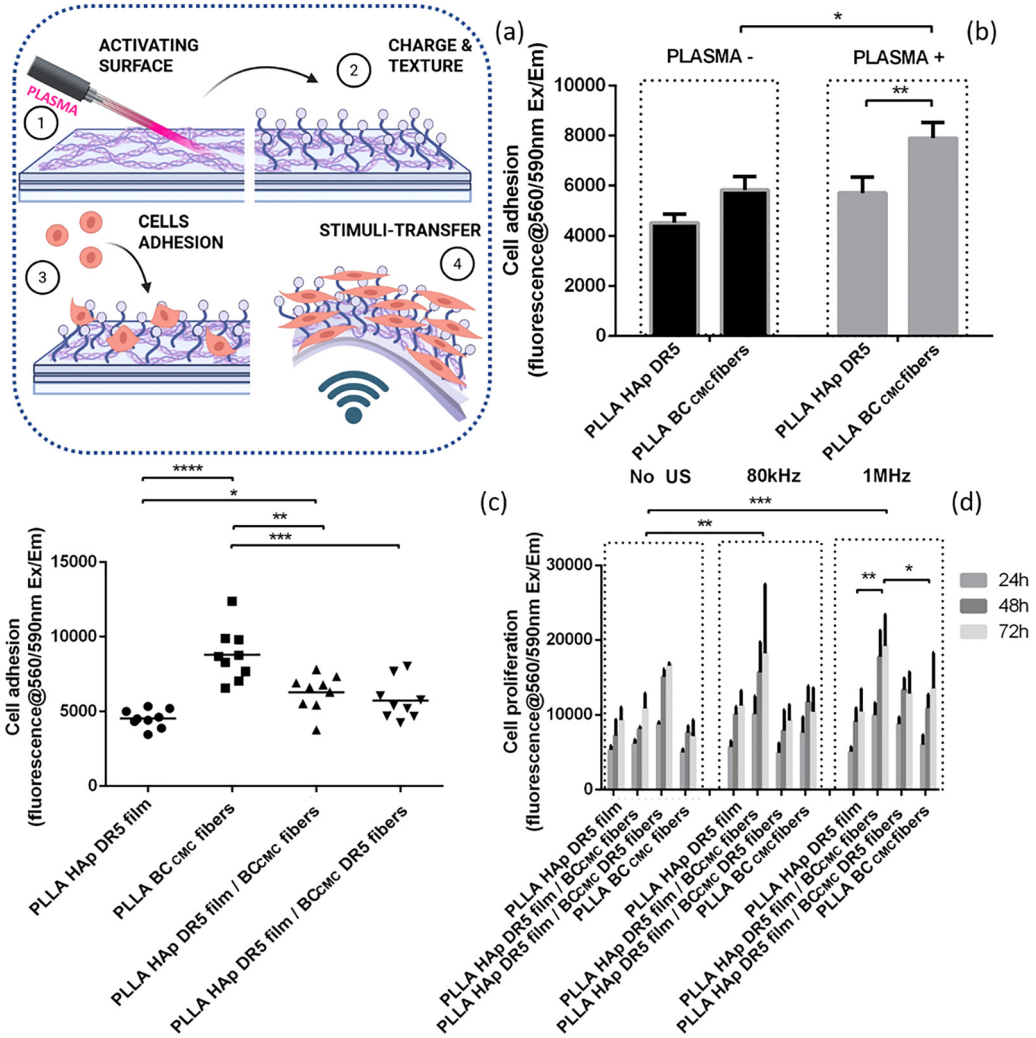

Fig. 6 Interactivity of two-layered films and ultrasound stimulated HaCaT cells growth. Toward effective interactions between materials surface and cells: 1-activating surface, 2- plasma induced surface changes, 3- enhancing cells adhesion and 4- effective stimuli transfer during piezostimlation (a), plasma- affected cell adhesion (for PLLA HAp DR5 film and PLLA BC_{CMC} fibres with and without plasma pre-treatment) (b), cell adhesion at plasma-modified surface of single-layer (PLLA HAp DR5 and PLLA BC_{CMC} fibres) and two-layered (PLLA HAp DR5/BC_{CMC} fibres and PLLA HAp DR5/BC_{CMC} fibres DR5) materials (c), proliferation of cells at the surface of all single- and two- morphology materials without and with activation using 80 kHz or 1 MHz US (d), n = 3–9, *, **, *** and **** indicate $p < 0.05$, $p < 0.005$, $p < 0.001$ and $p < 0.0001$, respectively.

the fibrous morphology. Plasma treatment further amplified this effect ($p < 0.005$), consistent with increased hydrophilicity, higher densities of anionic functional groups, and tailored surface roughness (Fig. 5).

Comparative analysis of plasma-treated single- and two-layered structures revealed a clear advantage of hierarchical architectures (Fig. 6c). Two-layered materials supported significantly higher cell adhesion than single-morphology substrates, with the PLLA HAp DR5/BC_{CMC} fibres system showing the strongest enhancement ($p < 0.001$). Notably, randomly oriented fibres at the surface promoted greater cell adhesion than uniaxially aligned fibres, indicating a cellular preference for isotropic, ECM-like architectures.

To evaluate piezostimulation, cells adhered to the materials were exposed to ultrasound (US) at 80 kHz or 1 MHz. US activation promoted cell proliferation relative to non-stimulated controls (Fig. 6d), with the strongest effect observed for PLLA HAp DR5/BC_{CMC} fibres, which also exhibited the highest piezoelectric output (Fig. 4). However, no significant difference was observed between 80 kHz and 1 MHz stimulation, suggesting a possible saturation of the proliferative response. Under 1 MHz stimulation, proliferation on this two-layered material was significantly higher than on single-layer PLLA HAp DR5 films ($p < 0.005$) and PLLA BC_{CMC} fibres ($p < 0.05$), consistent with frequency-dependent enhancement of electromechanical coupling.

In contrast, the PLLA HAp DR5/BC_{CMC} DR5 system with uniaxially aligned fibres did not show increased proliferation upon US activation, despite high baseline cell growth. This behaviour is attributed to reduced interfacial adhesion and weaker electromechanical coupling, resulting in lower piezoelectric output (Fig. 4), in agreement with previous reports on

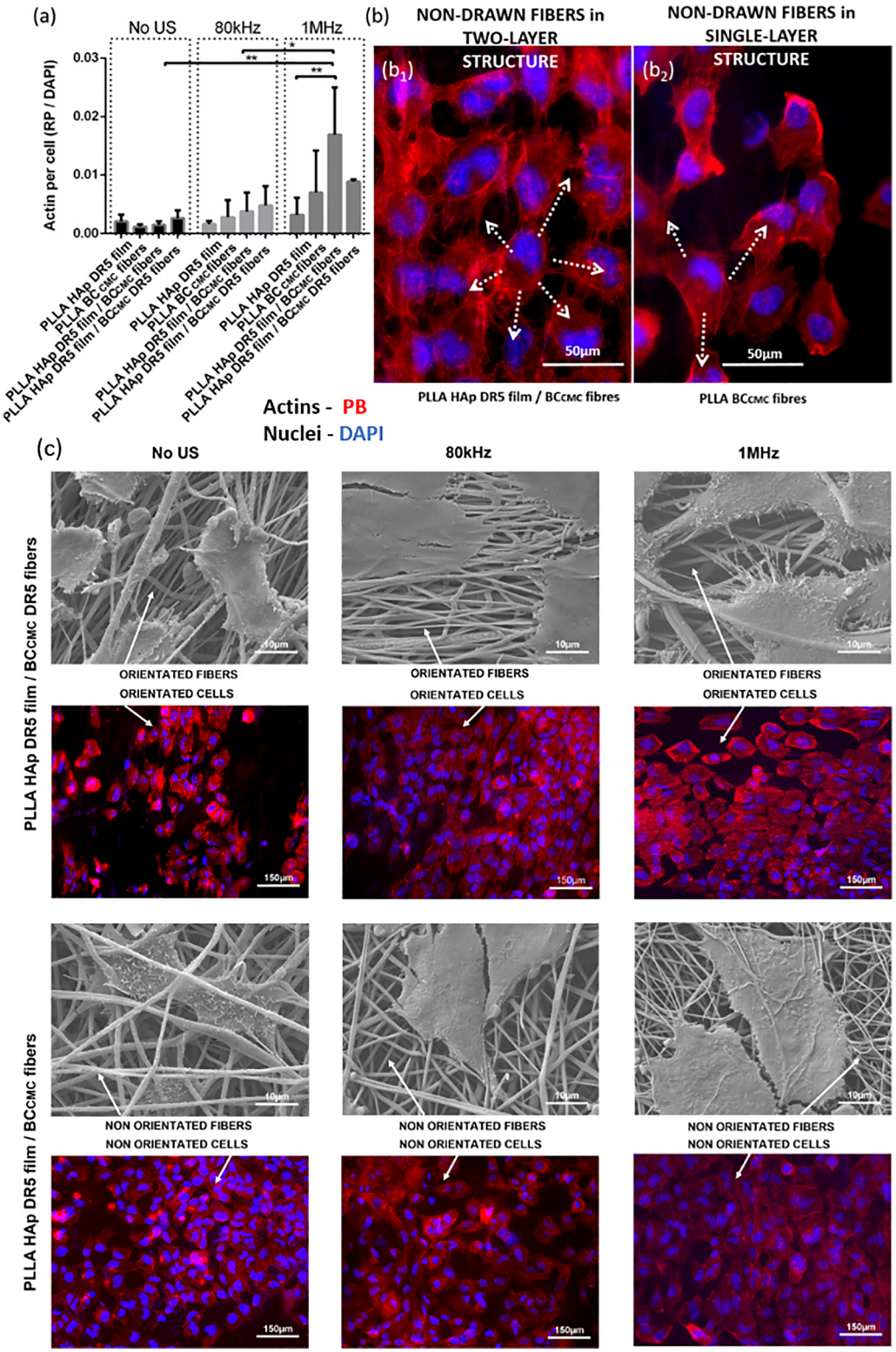

Fig. 7 Interactivity of two-layered films and effect to HaCaT cells cytoskeleton. Quantification of actin filaments in cells at the surface of films following activation by US (80 kHz or 1 MHz) (a), actin formation in stimulated cells in single- and two- layered PLLA fibrous structures (b), cell morphology and actin filaments in cells stimulated at the surface of PLLA HAp DR5 film/BC_{CMC} DR5 fibers (orientated fibers, orientated cells) and PLLA HAp DR5 film/ BC_{CMC} fibers (non-orientated fibers, non-orientated cells) without ultrasound (No US), and with 80 kHz and 1 MHz ultrasound stimulation (c), * and ** indicate $p < 0.05$ and $p < 0.005$, respectively.

oriented piezoelectric PLLA systems. Importantly, plasma-activated interlayer adhesion remained stable under prolonged aqueous exposure and repeated US stimulation (as confirmed with cross section investigation (Fig. S9)), preventing delamination under dynamic loading conditions.

Testing controls confirmed no significant increase in cell proliferation observed when cultured on standard tissue culture plate without piezoelectric material or on non-piezoelectric material (Fig. S10), indicating that US alone did not drive the cellular response. Temperature changes during stimulation remained within physiologically relevant limits, as previously reported,[13] indicating that the observed effects are unlikely to originate from thermal mechanisms and are primarily attributed to electromechanical coupling induced by ultrasound-driven deformation of the piezoelectric layers.

Cytoskeletal organization and morphological response to piezostimulation

Differences in piezoelectric response and cell proliferation were reflected in cytoskeletal organization. US stimulation enhanced actin filament formation on all PLLA substrates, with a significantly stronger effect at 1 MHz compared to 80 kHz and non-stimulated controls (Fig. 7a). Fibrous surfaces promoted more pronounced actin organization than smooth films, with the strongest response observed on PLLA HAp DR5/BC_{CMC} fibres featuring randomly oriented fibres ($p < 0.001$), consistent with their superior electromechanical performance. The significant difference relative to 80 kHz indicates that actin filament organization appears to be more sensitive to the magnitude of the generated electrical stimulus, consistent with the established role of actin as a biological force sensor,[40] while cell proliferation is primarily governed by mechanical stimuli transmitted from the ultrasound-deformed bilayer to the cells growing on its surface (Fig. S11).Cells on two-layered fibrous structures (Fig. 7b) exhibited increased filopodia density and enhanced cell–cell connectivity compared to single-layer fibrous mats (Fig. S12 and S13), indicating more efficient signal transfer at the cell–material interface. Fibre orientation further modulated cell morphology: uniaxially aligned fibres induced directional cell elongation and actin alignment, particularly under US stimulation, whereas randomly oriented fibres promoted isotropic spreading, infiltration into the fibrous network, and three-dimensional anchoring (Fig. 7c).

Unlike previously reported oriented piezoelectric PLLA systems that primarily promoted directional migration,[13] the present two-layered architectures combine enhanced adhesion, proliferation, and infiltration. This multifunctional response arises from interface-governed electromechanical coupling under US activation combined with an ECM-mimetic fibrous biointerface. The resulting output voltages remain within the physiological range relevant for wound healing,[41,42] while enabling efficient transfer of electromechanical signals to cells both at the surface and within the scaffold bulk.

Taken together, this work introduces a multilayer, architecture-driven design paradigm for piezoelectric biomaterials, in which direct interlayer coupling enables synergistic control of electromechanical response and biological interactivity. By integrating ultrasound-amplified electromechanical coupling with a bioinspired, ECM-mimetic fibrous surface, the two-layered PLLA scaffolds overcome a central limitation of earlier piezoelectric systems—the separation of directional cell guidance from proliferative stimulation. The resulting materials operate within physiologically relevant electric potential ranges while enabling efficient transfer of electromechanical signals to cells both at the surface and within the scaffold bulk. Importantly, this amplification strategy arises from structural design rather than filler loading, rendering it broadly applicable to other piezoelectric polymers and composite architectures. Beyond wound healing, mechanically activated multilayer piezoelectric scaffolds of this type define a promising frontier for regenerative medicine, dynamic tissue models, and electroactive biomaterial design, where hierarchical structure, spatially resolved stimulation, and biological function must be simultaneously orchestrated.

Although demonstrated here using PLLA, the proposed interface-governed electromechanical coupling mechanism is broadly applicable to other shear-active piezoelectric polymers and multilayer soft electronic systems. Plasma treatment represents one of several possible interfacial chemistries capable of enabling this effect, highlighting the general relevance of chemically programmed interfaces as functional elements in bioinspired electromechanical materials.

Conclusions

Direct coupling of piezoelectric PLLA layers enabled by plasma surface modification induces efficient electromechanical coupling under ultrasound activation and represents a practical and versatile strategy for tailoring the piezoelectric response of this polymer. The generated electromechanical stimuli are effectively transferred to cells adhered to plasma-modified surfaces, particularly in architectures featuring a porous fibrous top layer that closely mimics the microstructure of the extracellular matrix. By combining enhanced piezoelectric activation with bioinspired surface design, the proposed multilayer approach provides an effective route to tailoring the interactivity of piezoelectric biomaterials, with strong potential for future applications in bioelectronics, regenerative medicine, and tissue engineering. More broadly, this work positions chemically engineered interfaces as a new design axis for electromechanical materials, where function emerges from interfacial coupling rather than bulk optimization—mirroring the interface-centric logic of biological mechanotransduction.

Author contributions

MŽ – conceptualization, methodology, investigation, writing – original draft; LG – formal analysis, writing – review & editing; MSS – investigation, methodology; IJ – methodology; SG – investigation, writing – review & editing; AR – formal analysis, writing – review & editing; MS – writing – review & editing,

funding acquisition; MV – conceptualization, writing – review & editing, funding acquisition, supervision.

Conflicts of interest

There are no conflicts to declare.

Data availability

Data for this article are available at Zenodo at [https://doi.org/10.5281/zenodo.18256142].

Supplementary information: description of experimental procedures and characterization methods as well as additional data supporting this work. See DOI: https://doi.org/10.1039/d6mh00147e.

Acknowledgements

This work has been supported by Slovenian Research and Innovation Agency (ARIS) within grants PR-12591, J3-4531 and N2-0388 and research programs P2-0091 and P1-0125. Authors would like to acknowledge David Fabijan, Lucija Bučar and Blaž Jaklič from Advanced Materials Department, Jožef Stefan Institute, for DSC, XRD and piezoelectric measurements. We acknowledge CMS-Biocev (''Biophysical techniques, Crystallization, Diffraction, Structural mass spectrometry'') of CIISB, Instruct-CZ Centre, supported by MEYS CR (LM2023042) and CZ.02.1.01/0.0/0.0/18_046/0015974. The illustrations are made using BioRender software.

Notes and references

1 D. Nepal, S. Kang, K. M. Adstedt, K. Kanhaiya, M. R. Bockstaller, L. C. Brinson, M. J. Buehler, P. V. Coveney, K. Dayal, J. A. El-Awady, L. C. Henderson, D. L. Kaplan, S. Keten, N. A. Kotov, G. C. Schatz, S. Vignolini, F. Vollrath, Y. Wang, B. I. Yakobson, V. V. Tsukruk and H. Heinz, Hierarchically structured bioinspired nanocomposites, *Nat. Mater.*, 2023, **22**, 18–35, DOI: 10.1038/s41563-022-01384-1.

2 A. Saraswathibhatla, D. Indana and O. Chaudhuri, Cell–extracellular matrix mechanotransduction in 3D, *Nat. Rev. Mol. Cell Biol.*, 2023, **24**, 494–516, DOI: 10.1038/s41580-023-00583-1.

3 A. Teixeira do Nascimento, P. R. Stoddart, T. Goris, M. Kael, R. Manasseh, K. Alt, J. Tashkandi, B. C. Kim and S. E. Moulton, Stimuli-Responsive Materials for Biomedical Applications, *Adv. Mater.*, 2025, **37**(36), e07559, DOI: 10.1002/adma.202507559.

4 H. Xin, D. A. Maruf, F. Akin-Ige and S. Amin, Stimuli-responsive hydrogels for skin wound healing and regeneration, *Emergent Mater.*, 2025, **8**, 1339–1356, DOI: 10.1007/s42247-024-00930-8.

5 F. Mottaghitalab and M. Farokhi, Stimulus-responsive biomacromolecule wound dressings for enhanced drug delivery in chronic wound healing: A review, *Int. J. Biol. Macromol.*, 2024, **281**(Part 4), 136496, DOI: 10.1016/j.ijbiomac.2024.136496.

6 D. L. Miller, N. B. Smith, M. R. Bailey, G. J. Czarnota, K. Hynynen and I. R. S. Makin, Overview of therapeutic ultrasound applications and safety considerations, *J. Ultrasound Med.*, 2012, **31**(4), 623–634, DOI: 10.7863/jum.2012.31.4.623.

7 A. Cafarelli, A. Marino, L. Vannozzi, J. Puigmartí-Luis, S. Pané, G. Ciofani and L. Ricotti, Piezoelectric Nanomaterials Activated by Ultrasound: The Pathway from Discovery to Future Clinical Adoption, *ACS Nano*, 2021, **15**(7), 11066–11086, DOI: 10.1021/acsnano.1c03087.

8 R. Schönlein, P. Bhattarai, M. Raef, X. Larrañaga, A. Poudel, M. Biggs, R. Aguirresarobe and J. M. Ugartemendia, Piezoelectric polylactic acid-based biomaterials: fundamentals, challenges and opportunities in medical device design, *Biomaterials*, 2026, **324**, 123522, DOI: 10.1016/j.biomaterials.2025.123522.

9 M. Smith and S. Kar-Narayan, Piezoelectric polymers: theory, challenges and opportunities, *Int. Mater. Rev.*, 2022, **67**(1), 65–88, DOI: 10.1080/09506608.2021.1915935.

10 P. De Santis and A. J. Kovacs, Molecular Conformation of Poly (S-lactic Acid), *Biopolymers*, 1968, **6**(3), 299–306, DOI: 10.1002/bip.1968.360060305.

11 B. Lotz, Crystal polymorphism and morphology of polylactides, *Advances in Polymer Science*, Springer, New York LLC, 2018, vol. 279, pp. 273–302.

12 H. Wang, J. Zhang and K. Tashiro, Phase Transition Mechanism of Poly(l-lactic acid) among the α, δ, and β Forms on the Basis of the Reinvestigated Crystal Structure of the β Form, *Macromolecules*, 2017, **50**, 3285–3300, DOI: 10.1021/acs.macromol.7b00272.

13 M. Vukomanović, L. Gazvoda, M. Kurtjak, M. Maček-Kržmanc, M. Spreitzer, Q. Tang, J. Wu, H. Ye, X. Chen, M. Mattera, J. Puigmartí-Luis and S. V. Pane, Filler-Enhanced Piezoelectricity of Poly-L-Lactide and Its Use as a Functional Ultrasound-Activated Biomaterial, *Small*, 2023, **19**(35), 2301981, DOI: 10.1002/smll.202301981.

14 L. Udovč, M. Spreitzer and M. Vukomanović, Towards hydrophilic piezoelectric poly-L-lactide films: optimal processing, post-heat treatment and alkaline etching, *Polym. J.*, 2020, **52**, 299–311, DOI: 10.1038/s41428-019-0281-5.

15 M. Smith, T. Chalklen, C. Lindackers, Y. Calahorra, C. Howe, A. Tamboli, D. V. Bax, D. J. Barrett, R. E. Cameron, S. M. Best and S. Kar-Narayan, *et al.*, Poly- l -Lactic Acid Nanotubes as Soft Piezoelectric Interfaces for Biology: Controlling Cell Attachment via Polymer Crystallinity, *ACS Appl. Bio Mater.*, 2020, **3**(4), 2140–2149, DOI: 10.1021/acsabm.0c00012.

16 L. Gazvoda, M. Perišić Nanut, M. Spreitzer and M. Vukomanović, Antimicrobial activity of piezoelectric polymer: piezoelectricity as the reason for damaging bacterial membrane, *Biomater. Sci.*, 2022, **10**, 4933–4948, DOI: 10.1039/D2BM00644H.

17 A. Handler and D. D. Ginty, The mechanosensory neurons of touch and their mechanisms of activation, *Nat. Rev. Neurosci.*, 2021, **22**, 521–537, DOI: 10.1038/s41583-021-00489-x.

18 F. Jiang, Y. Shan, J. Tian, L. Xu, C. Li, F. Yu, X. Cui, C. Wang, Z. Li and K. Ren, Poly(L-Lactic Acid) Nanofiber-Based Multilayer Film for the Electrical Stimulation of Nerve Cells, *Adv.*

Mater. Interfaces, 2023, **10**(17), 2202474, DOI: 10.1002/admi.202202474.

19 R. Das, E. J. Curry, T. T. Le, G. Awale, Y. Liu, S. Li, J. Contreras, C. Bednarz, J. Millender, X. Xin, D. Rowe, S. Emadi a, K. W. H. Lo and T. D. Nguyen, Biodegradable nanofiber bone-tissue scaffold as remotely-controlled and self-powering electrical stimulator, *Nano Energy*, 2020, **76**, 105028, DOI: 10.1016/j.nanoen.2020.105028.

20 R. Das, T. T. Le, B. Schiff, M. T. Chorsi, J. Park, P. Lam, A. Kemerley, A. M. Supran, A. Eshed, N. Luu, N. G. Menon, T. A. Schmidt, H. Wang, Q. Wu, M. Thirunavukkarasu, N. Maulik and T. D. Nguyen, Biodegradable piezoelectric skin-wound scaffold, *Biomaterials*, 2023, **301**, 122270, DOI: 10.1016/j.biomaterials.2023.122270.

21 A. B. D. Cassie and S. Baxter, Wettability of porous surfaces, *Trans. Faraday Soc.*, 1944, **40**, 546–551, DOI: 10.1039/TF9444000546.

22 W. Zhang, M. Liu, Y. Liu, R. Liu, F. Wei, R. Xiao and H. Liu, *et al.*, 3D porous poly(l-lactic acid) foams composed of nanofibers, nanofibrous microsheaves and microspheres and their application in oil-water separation, *J. Mater. Chem. A*, 2015, **3**(26), 14054–14062, DOI: 10.1039/C5TA02759D.

23 M. Vukomanović, M. Zabcic, M. S. Salehidashtbayaz, I. Junkar and M. Spreitzer, A multi-layered structure comprising an organic piezoelectric material, a method for the preparation thereof and a biodegradable medical material, 2025, EPO, EP25218521.0.

24 S. Zhang, H. Zhang, J. Sun, N. Javanmardi, T. Li, F. Jin, Y. He, G. Zhu, Y. Wang, T. Wang and Z.-Q. Feng, A review of recent advances of piezoelectric poly-L-lactic acid for biomedical applications, *Int. J. Biol. Macromol.*, 2024, **276**(Part 1), 133748, DOI: 10.1016/j.ijbiomac.2024.133748.

25 M. Zhao, B. Song, J. Pu, T. Wada, B. Reid, G. Tai, F. Wang, A. Guo, P. Walczysko, Y. Gu, T. Sasaki, A. Suzuki, J. V. Forrester, H. R. Bourne, P. N. Devreotes, C. D. McCaig and J. M. Penninger, Electrical signals control wound healing through phosphatidylinositol-3-OH kinase-γ and PTEN, *Nature*, 2006, **442**, 457–460, DOI: 10.1038/nature04925.

26 U. Jančič, I. Nacu, L. Verestiuc, F. Rancan and S. Gorgieva, Bioactive bacterial nanocellulose membranes for non-surgical debridement and infection prevention in burn wound healing, *Carbohydr. Polym. Technol. Appl.*, 2025, **10**, 100762, DOI: 10.1016/j.ijbiomac.2024.131329.

27 C. Ma, L. Wang, A. Nikiforov, Y. Onyshchenko, P. Cools, K. K. Ostrikov, N. De Geyter and R. Morent, Atmospheric-pressure plasma assisted engineering of polymer surfaces: From high hydrophobicity to superhydrophilicity, *Appl. Surf. Sci.*, 2021, **535**, 147032, DOI: 10.1016/j.apsusc.2020.147032.

28 F. Awaja, M. Gilbert, G. Kelly, B. Fox and P. J. Pigram, Adhesion of polymers, *Prog. Polym. Sci.*, 2009, **34**(9), 948–968, DOI: 10.1016/j.progpolymsci.2009.04.007.

29 I. Junkar, G. Primc, T. Mivsek, M. Resnik, J. Kovac, A. Sever Skapin, A. Podgornik and M. Mozetic, Plasma Treatment-Promising Tool for Preparation of Disposable Monolithic Columns, *J. Anal. Bioanal. Technol.*, 2015, **6**, 253, DOI: 10.4172/2155-9872.1000253.

30 M. Koga, Y. Yamamichi, Y. Nomoto, M. Irie, T. Tanimura and T. Yoshinaga, Rapid Determination of Anionic Surfactants by Improved Spectrophotometric Method Using Methylene Blue, *Anal. Sci.*, 1999, **15**(6), 563–568, DOI: 10.2116/analsci.15.563.

31 K. Takahashi, D. Sawai, T. Yokoyama, T. Kanamoto and S. H. Hyon, Crystal transformation from the α- to the β-form upon tensile drawing of poly(L-lactic acid), *Polymer*, 2004, **45**(14), 4969–4976, DOI: 10.1016/j.polymer.2004.03.108.

32 S. Wanwong, W. Sangkhun and P. Jiamboonsri, Electrospun Cyclodextrin/Poly(L-lactic acid) Nanofibers for Efficient Air Filter: Their PM and VOC Removal Efficiency and Triboelectric Outputs, *Polymers*, 2023, **15**(3), 722, DOI: 10.3390/polym15030722.

33 S. Li, X. Liu, R. Li and Y. Su, Shear deformation dominates in the soft adhesive layers of the laminated structure of flexible electronics, *Int. J. Solids Struct.*, 2017, **110–111**, 305–314, DOI: 10.1016/j.ijsolstr.2016.12.006.

34 E. Gorgun, Ultrasonic testing and surface conditioning techniques for enhanced thermoplastic adhesive bonds, *J. Mech. Sci. Technol.*, 2024, **38**, 1227–1236, DOI: 10.1007/s12206-024-0218-6.

35 M. Ali, M. Shahid, H. A. K. Lodhi, D. Naseer and I. Sadiq, Interface Adhesion Strength of Adhesive-Bonded Materials Using Ultrasonic Technique, *J. Multidiscip. Res.*, 2019, **11**(1), 8–17.

36 M. Chen, P. K. Patra, M. L. Lovett, D. L. Kaplan and S. Bhowmick, Role of electrospun fibre diameter and corresponding specific surface area (SSA) on cell attachment, *J. Tissue Eng. Regen. Med.*, 2009, **3**, 269–279, DOI: 10.1002/term.163.

37 J. Nam, Y. Huang, S. Agarwal and J. Lannutti, Improved cellular infiltration in electrospun fiber via engineered porosity, *Tissue Eng.*, 2007, **13**, 2249–2257, DOI: 10.1089/ten.2006.0306.

38 M. M. Abolhasani, M. Naebe, K. Shirvanimoghaddam, H. Fashandi, H. Khayyam, M. Joordens, A. Pipertzis, S. Anwar, R. Berger, G. Floudas, J. Michels and K. Asadi, Thermodynamic approach to tailor porosity in piezoelectric polymer fibers for application in nanogenerators, *Nano Energy*, 2019, **62**, 594–600, DOI: 10.1016/j.nanoen.2019.05.044.

39 M. Hassanpour Amiri and K. Asadi, How Porosity Affects the Performance of Piezoelectric Energy Harvesters and Sensors, *Adv. Phys. Res.*, 2023, **2**(2), 2200042, DOI: 10.1002/apxr.202200042.

40 V. E. Galkin, A. Orlova and E. H. Egelman, Actin filaments as tension sensors, *Curr. Biol.*, 2012, **22**(3), R96–R101, DOI: 10.1016/j.cub.2011.12.010.

41 R. Luo, Y. Liang, H. Feng, Y. Chen, X. Jiang, Z. Zhang, J. Liu, Y. Bai, J. Xue, S. Chao, Y. Xi, X. Liu, E. Wang, D. Luo, Z. Li and J. Zhang, Reshaping the Endogenous Electric Field to Boost Wound Repair via Electrogenerative Dressing, *Adv. Mater.*, 2023, **35**(16), 2208395, DOI: 10.1002/adma.202208395.

42 K. Kapat, Q. T. H. Shubhra, M. Zhou and S. Leeuwenburgh, Piezoelectric Nano-Biomaterials for Biomedicine and Tissue Regeneration, *Adv. Funct. Mater.*, 2020, **30**(44), 1909045, DOI: 10.1002/adfm.201909045.

